



EEG feature fusion for motor imagery: A new robust framework towards stroke patients rehabilitation



Noor Kamal Al-Qazzaz^a, Zaid Abdi Alkareem Alyasseri^{b,c,*}, Karrar Hameed Abdulkareem^d, Nabeel Salih Ali^f, Mohammed Nasser Al-Mhiqani^e, Christoph Guger^g

^a Department of Biomedical Engineering, Al-Khwarizmi College of Engineering, University of Baghdad, Baghdad, 47146, Iraq

^b Center for Artificial Intelligence Technology, Faculty of Information Science and Technology, Universiti Kebangsaan Malaysia, 43600, Bangi, Selangor, Malaysia

^c ECE Department-Faculty of Engineering, University of Kufa, P.O. Box 21, Najaf, Iraq

^d College of Agriculture, Al-Muthanna University, Samawah, 66001, Iraq

^e Information Security and Networking Research Group (InFORSNET), Faculty of Information and Communication Technology, Universiti Teknikal Malaysia Melaka, Durian Tunggal, 76100, Malaysia

^f Information Technology Research and Development Centre/ University of Kufa, Kufa, P.O. Box (21), Najaf Governorate, Iraq

^g G.tec Medical Engineering GmbH, Schiedlberg, Austria

ARTICLE INFO

Keywords:

EEG
Brain-computer interfaces
Feature extraction
Feature fusion
Motor imagery
Stroke rehabilitation

ABSTRACT

Stroke is the second foremost cause of death worldwide and is one of the most common causes of disability. Several approaches have been proposed to manage stroke patient rehabilitation such as robotic devices and virtual reality systems, and researchers have found that the brain-computer interfaces (BCI) approaches can provide better results. Therefore, the most challenging tasks with BCI applications involve identifying the best technique(s) that can reveal the neuron stimulus information from the patients' brains and extracting the most effective features from these signals as well. Accordingly, the main novelty of this paper is twofold: propose a new feature fusion method for motor imagery (MI)-based BCI and develop an automatic MI framework to detect the changes pre- and post-rehabilitation. This study investigated the electroencephalography (EEG) dataset from post-stroke patients with upper extremity hemiparesis. All patients performed 25 MI-based BCI sessions with follow up assessment visits to examine the functional changes before and after EEG neurorehabilitation. In the first stage, conventional filters and automatic independent component analysis with wavelet transform (AICA-WT) denoising technique were used. Next, attributes from time, entropy and frequency domains were computed, and the effective features were combined into time–entropy–frequency (TEF) attributes. Consequently, the AICA-WT and the TEF fusion set were utilised to develop an AICA-WT-TEF framework. Then, support vector machine (SVM), k-nearest neighbours (kNN) and random forest (RF) classification technique were tested for MI-based BCI rehabilitation. The proposed AICA-WT-TEF framework with RF classifier achieves the best results compared with other classifiers. Finally, the proposed framework and feature fusion set achieve a significant performance in terms of accuracy measures compared to the state-of-the-art. Therefore, the proposed methods could be crucial for improving the process of automatic MI rehabilitation and are recommended for implementation in real-time applications.

1. Introduction

Stroke is a brain injury condition due to cerebral circulation disorder and has critically threatened human health for long periods [1]. A stroke is ranked second among the 10 leading causes of death worldwide

according to the World Health Organization (WHO), and crude mortality rates indicate 85 deaths from stroke per 100,000 people [2]. Cerebral stroke clearly interrupts and reorganises functioning brain networks near and far from the lesion [3]. The most common form of ischemic stroke has a worldwide impact of approximately 11.6 million

* Corresponding author. Center for Artificial Intelligence Technology, Faculty of Information Science and Technology, Universiti Kebangsaan Malaysia, 43600, Bangi, Selangor, Malaysia.

E-mail addresses: noorbme@kecbu.uobaghdad.edu.iq (N.K. Al-Qazzaz), zaid.alyasseri@uokufa.edu.iq (Z.A.A. Alyasseri), khak9784@mu.edu.iq (K.H. Abdulkareem), nabeel@uokufa.edu.iq (N.S. Ali), almohaiqny@gmail.com (M.N. Al-Mhiqani), guger@gtec.at (C. Guger).

new cases annually [4]. Hemiparesis involves complete paralysis or paralysis of one side of the body, including the arm, leg, foot, and hand, and is one of the most deficient engine damage caused by ischemic stroke. Only 35% of patients recover sufficient hand-motor function for everyday activities after six months of experiencing the stroke [5]. Moreover, stroke survivors are impaired by different disabilities that contribute to visual and cognitive impairment [5].

Those disabilities have a huge effect on day-to-day activities [7]. Efficient treatment, therapy and rehabilitation for stroke patients have been the focus of recent research. Therapy and rehabilitation aim to help the brain restore neural connections and compensate for disrupted circuits. However, the selection of the best treatment can take weeks and is not yet observable in an objective way [8]. Patient's medical condition and changes in brain activities arise quickly and may be detected via electroencephalogram (EEG) signals [9].

The EEG is a non-invasive, safe neurophysiological tool that can record brain activities at low cost [10]; but processing the collected information that properly describes the state of the brain is necessary [11]. Some researchers used EEG signals to diagnose individuals with ischemic stroke [3] by investigating and extracting significant variables using a brain computer interface (BCI) for stroke rehabilitation [13–16]. Various studies [17,18] confirmed that the changes in brain function deterioration through EEG patterns during stroke are almost immediate; for example, high-frequency waves are attenuated, slow-frequency waves become dominant and brain waves activities exhibit asymmetry [3].

To detect and identify brain characteristics and evaluate the EEG signal variable being reviewed, recognising the most prominent marks from EEG signals is vital [8]. From the clinical perspective, the neurologist reads the EEG signal of a post-stroke patient by observing wave rhythms, amplitudes, asymmetries, changes in magnitudes, the presence of waves and the ratio between waves [19].

Nevertheless, various types of artifacts may distort the recorded wave activities [20]. These artifacts can usually imitate or superimpose the pathological behaviour of the brain [21]. Furthermore, EEG frequencies may be intersected by major artifacts that clash with the EEG, such as eye blinks, ocular movements, cardiac artifacts, muscle activities, and power line interference noise [19]. The presence of noise therefore makes it difficult to classify EEG signals [22].

The extraction of relevant data from EEG recordings is vital to correctly understand and analyse the required mental functions. Moreover, visual inspection and manual artifact extraction takes time, is difficult when dealing with extensive EEG information, cannot be processed in real time and is susceptible to human prejudice [23,24]. Consequently, preprocessing and feature extraction and classification are the key steps during the extraction of relevant information from EEG signals [25]. Different techniques have been used to analyse artifacts that affect EEG recording and interpretation for pathological activities accurately, including epoch rejection [26]; regression techniques [27] and blind source separation (BSS) [28]. Several studies used wavelet (WT) as a time-frequency analysis denoising technique [16,24]; others employed WT to evaluate relevant EEG signal variables for identifying the independent eye blink artifactual components in post-stroke patients as a decomposition method [16,29]. The study in [30] used WT to systematically evaluate the effectiveness of ocular artifact removal.

The extraction of relevant features for EEG data classification is a vital stage [31–33]. This situation is because the feature extraction stage has a major effect on the classification efficiency of the system [34]. If the features extracted are not expressive for a specific case, then the classification output is unacceptable. In these cases, the classification technique can be extremely ideal to the problem but the method cannot yield good classification results because of insufficient features. Therefore, extracting acceptable features from EEG signals is required to reach optimal classification performance [35]. Many researchers have investigated the properties of waves in stroke patients with a particular frequency [36].

In this study, the conventional filtering and AICA-WT technique were applied to denoise the EEG dataset. Attributes from time, entropy and frequency domains were extracted to characterise the EEG of the MI-based BCI. These features were selected according to previous studies that showed their usefulness in distinguishing different mental tasks like those for AD patients' EEGs [37–39]. Attributes from time, entropy and frequency domains were computed and the effective features were combined into time–entropy–frequency (TEF) attributes to illustrate the brain responses to MI-based BCI rehabilitation. Consequently, the AICA-WT and the TEF fusion set were utilised to develop an AICA-WT-TEF framework. Finally, the performances of support vector machine (SVM), k-nearest neighbours (kNN), and random forest (RF) classifiers were tested on the features individually and on the TEF fusion set. The proposed AICA-WT-TEF framework may be crucial for improving the automatic left or right MI-based EEG signals classification from stroke patients' rehabilitation.

This paper is organised as follows. Section 2 discusses related works about stroke patients' rehabilitation using EEG signals. Section 3 presents the feature extraction methods. Section 4 explains the proposed method. Section 5 presents the results and discussion. Finally, the conclusions and future works are described in Section 6.

2. Related works

According to [40]; even a 0.1% increase in the accuracy of classification in the medical context can be vital. Thus, our study seeks to optimize the accuracy of the MI classification task from two aspects: preprocessing (denoising) and feature extraction. Consequently, the proposed method is expected to make an important contribution to the stroke rehabilitation domain.

This work complements other efforts, expands the research direction on the classification of left or right MI-based EEG signals for stroke patients' rehabilitation that mainly focus on the enhancement of the recorded EEG signals, and extracts and investigates the EEG features that identify the stroke patients comparing control subjects. An EEG signal has many undesired characteristics such low signal-to-noise ratio (SNR), weak signal and high sensitivity to noise. In fact, the MI task for the right hand may be identified as an MI task for the left-hand as MI is a process of imagining the movement of a part of your own body without really moving that body part [41,42]. Furthermore, an overall classification task exhibits poor performance given the overlapping issue among EEG features [43]. A denoising step must be included in the MI EEG data classification to deal with the aforementioned issue. An effective signal preprocessing is also recognised as critical to achieve high classification accuracy [44]. In addition, according to outcomes for [20,45]; combining more than one filter for denoising has shown significant influence on the improvement of MI classification accuracy. Regarding preprocessing, Castellanos et al. [46] proposed a WT-Enhanced ICA approach for decomposed independent components by the application of the WT threshold. The WT thresholds enable the detection of artifactual elements in the time–frequency domains to re-build the brain activity incorporated in such components.

From the feature extraction aspect, Fourier transformation and correlative time–frequency features were extracted from EEG data and compared along with their discriminatory power. In the work by Liu et al. [47]; classification accuracy is one of the challenges in recognising anisomeric motor imagery from EEG signals. Although numerous EEG studies suggested extracting features from the frequency domain, the classification accuracy was not effective [48,49]. A study in EEG-recognition analysis considered the combination of many domains, including the time and frequency domain attributes, as advisable to enhance classification accuracy [50]. Moreover, when features were only unimodally extracted, the acquired features are fairly simple and undoubtedly leads to insufficient EEG details, thereby affecting the overarching performance of classification [51]. Accordingly, feature fusion resolves the aforementioned problem [51]. However, many

Table 1
Related works.

Study	Denoising		Feature extraction		Classification
	Single filter	Multi-filters	Single domain	Multi-domains	
[44]	✓		✓		✓
[52]	✓		✓		✓
[53]	✓		✓		✓
[54]	✓		✓		✓
[55]	✓		✓		✓
[56]	✓		✓		✓
[57]	✓		✓		✓
[45]		✓	✓		✓
Proposed work		✓	✓		✓

studies have addressed the problem of MI EEG stroke patients' data analysis. Existing research have also highlighted three main directions: denoising, feature extraction and classification stage as listed in Table 1.

According Table 1, all previous works have worked on MI classification tasks and provide a significant contribution in this direction. Different classifiers have also been employed, such as time-variant linear discriminant analysis (TVLDA) [45]; SVM [58]; LDA [57]; and Random forest (RF) [1]. Nevertheless, in terms of the preprocessing (denoising) stage, most existing studies used single conventional filtering except for [45]. Note that the accuracy rate scored by [45] has room for improvement. However, most previous MI EEG data analysis methods overlooked the advantages of adopting a combined filtering scheme for EEG signal denoising before implementing algorithms. In the context of a feature extraction phase, most existing studies have used various methods such as CSP or WT as feature extraction techniques that work within single domain characteristics. Nevertheless, the existing literature has never exhibited different feature extraction methods according to different domains where significant chances can be offered to improve the classification accuracy.

Our work aims to enhance the accuracy of classification from two perspectives. On the one hand, we adopt a multi-filters approach on the basis of conventional and AICA-WT techniques for denoising EEG signal data. On the other hand, we propose a TEF approach as a feature extraction method according to the fusion of three different domain features, specifically, the time, entropy and frequency domains.

To the author's best of knowledge, this work contributes to MI-based EEG signal classifications. The main contributions of this study are summarised as follows:

- Develop an automatic AICA-WT-TEF framework to detect the MI changes pre- and post-rehabilitation.
- Propose a denoising technique on the basis of multi-filters (conventional and AICA-WT) methods.
- Investigate the performance of different EEG features from various domains.
- Develop automated methods of feature extraction for EEG signals by proposing a new TEF feature fusion approach for MI-based BCI.
- Validate the performance of the AICA-WT-TEF framework within different classification models and state-of-the-art methods.

3. EEG features extraction

In this work, three types of EEG features are extracted: the time, entropy and frequency domain features. Identifying meaningful features from the recorded EEG data set is a crucial step in improving MI-based BCI rehabilitation. The features extracted from the EEG must describe the neurophysiological behaviour of the brain's embedded structures. Consequently, the effective set of features provide correct recognition of the BCI mental states. Thus, the choice of an appropriate set of features seems to have more impact on the filter classification performances than

the choice of a good classification model [21].

Therefore, several feature extraction techniques were performed and proposed for MI-based BCI rehabilitation in this work. These feature extraction techniques can be categorised into three groups specified below.

3.1. Time domain features

For the time domain features four features were extracted: the fractal dimension (FD), skewness (Skw) and kurtosis (Kurt), Hurst (Hur) and Hjorth parameters. The formulas for extracting these features are as follows:

1. Fractal Dimension (FD): Higuchi's fractal dimension (HFD) is a suitable approach for the analysis of EEG signals; this is because of its dependence on a binary sequence, and in most cases, the HFD is less sensitivity to noise [59]. Thus, this feature is applied for testing the EEG-based of MI BCI rehabilitation activity in stroke patients in this work.

$$x(n) = \frac{1}{n} * \sum_{m=1}^n x_m(n) \quad (1)$$

where n refers to a time interval and $x_m(n)$ is the average time series of the n values.

2. Skewness (Skw) and Kurtosis (Kurt): In this work (Skw) and (Kurt) are used according to [60].

$$e_i(n) = \sqrt{x_k(n)^2 + H(x_k(n)^2)} \quad (2)$$

Let $m_n = E(x - Ex)^2$ be the n th central moment of the Skw and Kurt distributions. Where $x_k(n)$ is the input EEG signals, k refers to a specific channel, H is the Hilbert transform. For that, we can extract Skw and Kurt as in Equations 3 and 4, respectively:

$$Skw = \frac{m_3}{(m_2)^{\left(\frac{3}{2}\right)}} \quad (3)$$

$$Kurt = \frac{m_4}{(m_2)^2} - 3 \quad (4)$$

3. Hurst (Hur): The hurst feature (Hur) is formulated as follows:

$$Hur = \log(R(n)/S(n))/\log(n) \quad (5)$$

where n refers to the EEG sample rate and $R(n)/S(n)$ refers to the corresponding rescaled value where $R(n)$ is the range of the first n cumulative deviations from the mean and $S(n)$ is the series sum of the first n standard deviations [61].

4. Hjorth Parameters: The Hjorth parameter is a feature consisting of mobility, activity, and complexity, which can be extracted from the time-domain feature [62]. The Hjorth parameter is defined as follows:

$$S1 = \frac{1}{n} \sum_{i=1}^n x_i^2 \quad (6)$$

where x denotes to the EEG signal, and $S1$ stands for a variance of x .

$$S2 = \frac{1}{n-1} \sum_{i=1}^{n-1} (x_{i+1} - x_i)^2 \quad (7)$$

$$S3 = \frac{1}{n-2} \sum_{i=1}^{n-2} ((x_{i+2} - x_{i+1}) - (x_{i+1} - x_i))^2 \quad (8)$$

$$ACy(f(i)) = Var(f(i)) = S1, \quad (9)$$

where ACy refers to the activity and Var refers to a variance.

$$Moy(f(i)) == \sqrt{\frac{ACy\left(\frac{df}{di}\right)}{ACy(f(i))}} = \sqrt{\frac{S2}{S1}}, \quad (10)$$

$$Coy(f(i)) = \frac{Moy\left(\frac{df}{di}\right)}{Moy(f(i))} = \sqrt{\frac{S3/S2}{S2/S1}}, \quad (11)$$

where Moy refers to a mobility and Coy refers to a complexity.

3.2. Entropy domain features

For entropy domain features, six different features are used in this work. The details of these features as follows:

1. Sample Entropy (SampEn): As SampEn is mainly independent of record length, it was introduced to reduce the bias and to eliminating self-matches that occurred in ApEn [63]. Thus, SampEn is computed using the algorithm presented in [64]; which is defined by:

$$SampEn(m, r, N) = -\ln \left[\frac{(A^m(r))}{(B^m(r))} \right] \quad (12)$$

where, $B^m(r)$ is the probability that two sequences will match for m points, whereas $A^m(r)$ is the probability that two sequences will match for $m + 1$ points.

2. Fuzzy Entropy (FuzEn): FuzEn is used to characterise different types of biomedical signals [63]. Furthermore, recent evidence suggests that FuzEn is a robust entropy estimator when there are missing samples in the biomedical signals being analyzed [65]. FuzEn can be calculated using the algorithm as in [65]; FuzEn is defined by:

$$FuzEn(m, n, r, N) = \ln \Phi m(n, r) - \ln \Phi m + 1(n, r) \quad (13)$$

where function Φm depends on the similarity degree Dij , m of the vectors $x_m(i)$ and $x_m(j)$ with a fuzzy function.

3. Tsallis Entropy (TsEn): TsEn entropies have been widely used to show the EEG changes estimated from time-domain-dependent entropy. For instance, TsEn has been derived from EEG of patients with Alzheimer's disease from related disorders and discriminate brain ischemia damage [63]. To quantify the uncertainty of a signal, we adopted entropy defined by Tsallis et al. [63,66].

$$S_T = \sum_{i=0}^n p(x_i) \ln_q \left(\frac{1}{p(x_i)} \right) = \frac{1 - \sum p^q(x_i)}{q-1} \quad (14)$$

where x_i are information events, $p(x_i)$ are the probabilities of x_i , and the q -logarithm function is defined as:

$$\ln_q(x) = \left(\frac{x^{(1-q)-1}}{(1-q)} \right) \forall x > 0, q \in \mathbb{R} \quad (15)$$

4. Improved Multiscale Permutation Entropy (impe): impe improves the reliability of the entropy estimations leading to more reliable and stable results and it is a promising technique to

characterise physiological changes affecting several temporal scales [67]. The impe can be calculated as in Equation (16).

$$impe(x, n, d) = \frac{1}{n} \sum_{m=1}^n PE(x) \quad (16)$$

where d is the embedding dimension.

5. Multiscale Fuzzy Entropy (MFE): Refer to the capability of the human brain to perform sophisticated cognitive tasks, in this study, and the nonlinear MFE was also used to analyse the recorded EEG signals. MFE method is based on the use of *FuzEn* values on multiple scales [68]; the EEG time series is denoted as $X = x(i): 1 \leq i \leq N$ and the coarse-grained time series $y(\tau)$ is constructed as $y_1(\tau), y_2(\tau), y_{\frac{N}{\tau}}(\tau)$, and can be computed based on Equation (17):

$$y_i(\tau) = 1/\tau \sum_{i=(j-1)\tau+1}^j x(i), 1 \leq j \leq N/\tau \quad (17)$$

where N is the length of time series and τ is a positive integer. The *FuzEn* of each coarse-grained time series can be computed as in [68]. Then, *MFE* is a function of scale factor τ , it can be computed by the following Equation (18):

$$MFE(X, \tau, m, n, r) = FE(y(\tau), m, n, r) \quad (18)$$

In this study, the parameters $\tau = 1$, $r = 0.25 \times SD$, and SD is the standard deviation of the original time series.

6. Refined Composite Multiscale Fuzzy Entropy (RCMFE): The input EEG signals, inclusive of the RCMFE, have been assessed by applying the non-linear entropy method, given that complex mental procedures may be undertaken by the brain.

The RCMFE is computed as in Equation (19):

$$RCMFE(x) = -\ln \left(\frac{\bar{\varphi}_t^{(m+1)}}{\bar{\varphi}_t^m} \right) \quad (19)$$

where m refers to the embedding dimension and x refers to the input EEG signals.

3.3. Frequency domain features

Two frequency features are used to measure the frequency domain features: mean frequency (meanF) and median frequency (MedF). The main purpose of using these features is to find the changes produced by different mental tasks such as mental disorders activity in the EEG signal [69].

1. Mean Frequency (meanF): In this part, the changes in EEG are investigated by using *meanF* to be an indicator of the general slowing of neural activity [69]. To compute the *meanF*, first, normalized the power spectral density (PSD) to the total power to get normalized $(PSD)_{norm}$ so that $(PSD)_{norm}(j) = PSD(j)/\sum_j (PSD)(j)$. Then, the *meanF* was then defined as in Equation (20).

$$meanF = \sum_j f(j) (PSD)_{norm}(j) \quad (20)$$

where j refers to the frequency bin and $f(j)$ refers to the mean frequency in Hz which is calculated for each frequency bin, and $(PSD)_{norm}(j)$ denotes the frequency power of the bin [70].

2. Median Frequency (MedF): Before calculating MedF, the EEG power spectra were estimated. First, the autocorrelation function of each EEG epoch was computed. The PSD was obtained as the Fourier transform of the autocorrelation vector. Thus, the spectral resolution

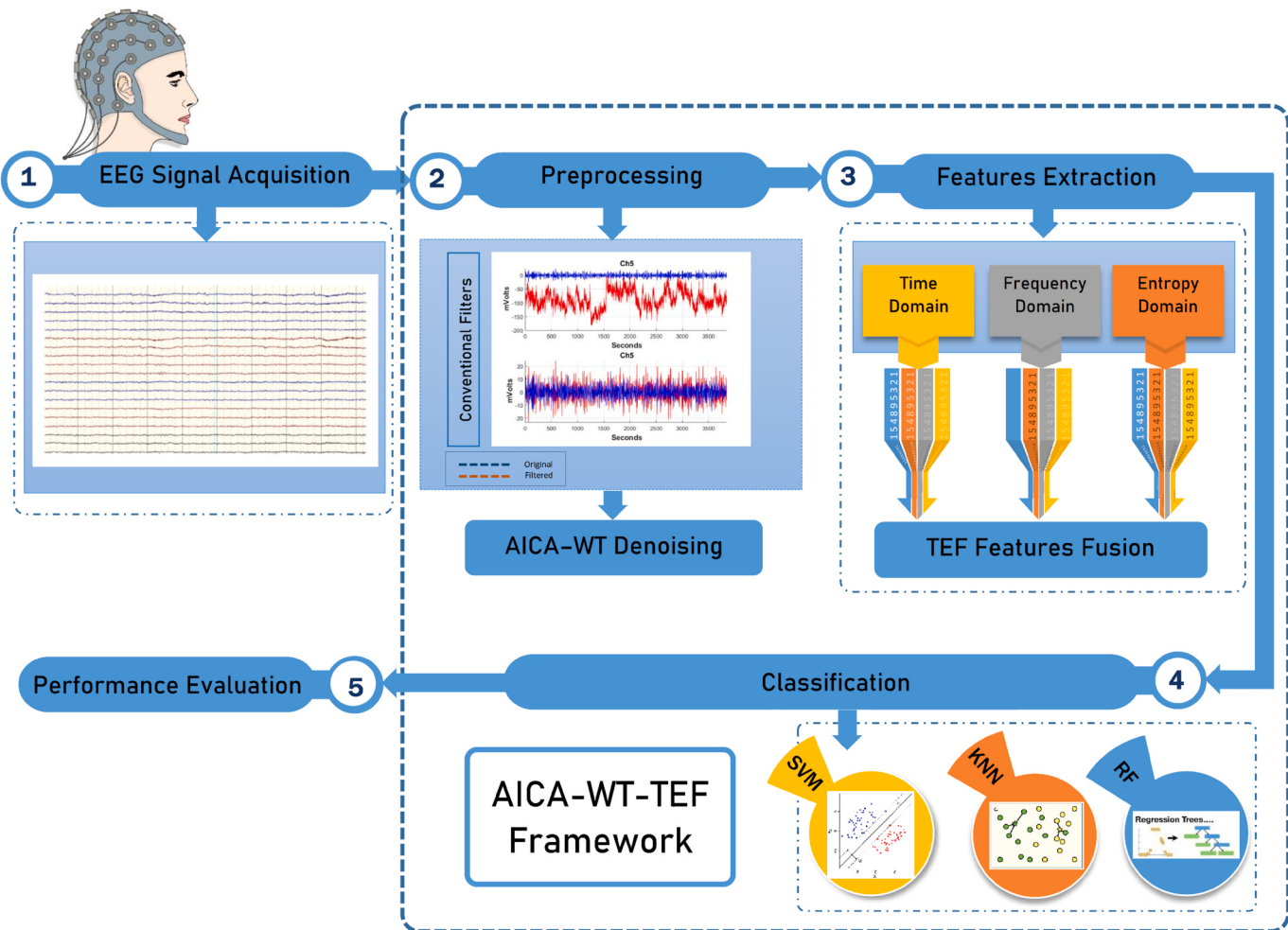


Fig. 1. Block diagram of the study including the proposed AICA-WT-TEF framework.

of this study equal to 0.05Hz. Then, MEG recordings were analyzed using the MedF, which is defined as the frequency that contains 50% of the PSD power [71]. Considering the 8–30Hz frequency band used in this study, the *MedF* was estimated from

$$MedF = 1/2 \left[\sum_{f=f_1}^{f_2} (PSD)f \right] = \sum_{f=f_1}^{f_2} (PSD)f \quad (21)$$

where *PSD* refers to power spectral density of each EEG signal, f_1 and f_2 refers the frequencies bands.

4. Proposed method

This study is intended to improve the MI-based BCI patient rehabilitation by applying three main stages: the preprocessing, feature extraction and classification stages. This work focused on the investigation of time, entropy and frequency domains towards an estimation of a robust TEF fusion approach to gain insights in the information from multiple domains. Features were combined to illustrate the changes in pre- and post-rehabilitation therapy over the brain regions. Therefore, to achieve satisfactory classification performances, this research involves a comparative study to represent the effect of individual time, entropy and frequency features and the combined TEF feature set. Accordingly, the AICA-WT-TEF framework is identified according to the combinations of denoised EEG signals after applying the AICA-WT denoising technique and the TEF feature set to help improve the MI-based BCI classification. The novel proposed AICA-WT-TEF framework is validated on a multi-

channel MI-based BCI EEG dataset. Fig. 1 shows the schematic block diagram of the proposed AICA-WT-TEF method.

4.1. EEG signal acquisition

In this work a standard EEG dataset has been used from g.tec medical engineering GmbH. More details about these dataset will explain in Section 5.1.

4.2. Preprocessing stage

The artifacts overlap the EEG frequency bands and may contaminate the human brain activities. Therefore, noise removal has a crucial role in EEG signal preprocessing. In this study, the preprocessing stage was performed by two sub-stages of the conventional filtering and the AICA-WT denoising techniques.

4.2.1. Conventional filtering

Two conventional filters were utilised initially for each channel of the recorded EEG dataset. Firstly, a butter-worth (*BW*) notch filter at (50 Hz) was applied to remove the power line interference noise, secondly, a bandpass filter (*BPF*) of frequencies around (8–30 Hz) was utilised to limit the band of the recorded EEG dataset [72].

4.2.2. AICA-WT denoising technique

(ICs) $s(t) = [s_1(t), \dots, s_n(t)]$ using *FastICA* algorithm proposed by [73]. The set $s(t)$ of n unknown components that were linearly mixed by

within matrix A and $x(t)$ is the set of n observations where $x(t) = [x_1(t), \dots, x_n(t)]$ [74–76]; represents the EEGs and are related to $s(t)$, t is the time, the ICA Equation is

$$x(t) = As(t) \quad (22)$$

The artifactual components *ICs* were tested using three parameters including Kurtosis (*Kurt*), skewness (*Skw*) and sample entropy (*SampEn*). For each *IC*, if these parameters exceeded the threshold of ± 1.2 , the *IC* were marked as critical and will be denoised using WT. The practical value of the threshold is selected through trial and error and according to previous studies [24,77,78]. The threshold value of ± 1.2 is not a drawback of *AICA* — *WT* technique as the artifactual *ICs* will not be rejected but will be denoised using the *WT* technique. Therefore, *WT* denoised the marked *ICs*, and then the enhanced components were returned back to the original EEG dataset [79,80].

4.2.3. The time-entropy-frequency (TEF) features fusion

To have more insight on the mental processes employed by the BCI users, a new biomarker was developed according to the combination of the extracted set of features. The characterised features with the three domains of time, entropy and frequency were selected on the basis of previous studies that illustrated their usefulness and effectiveness in discriminating the EEG signals [81–85]. Therefore, the fusion of a set of features using *HjAc* from the time domain, meanF from the frequency domain and improved multiscale permutation entropy (*impe*) features from the entropy domain towards developing the *TEF* features is important to obtain an efficient BCI model in terms of high accuracy recognition rates and more interpretable MI-based BCI rehabilitation.

4.3. Classification and performance measures

The last stage for identifying the BCI neurophysiological changes involves using the classification models. The goal of this stage is to

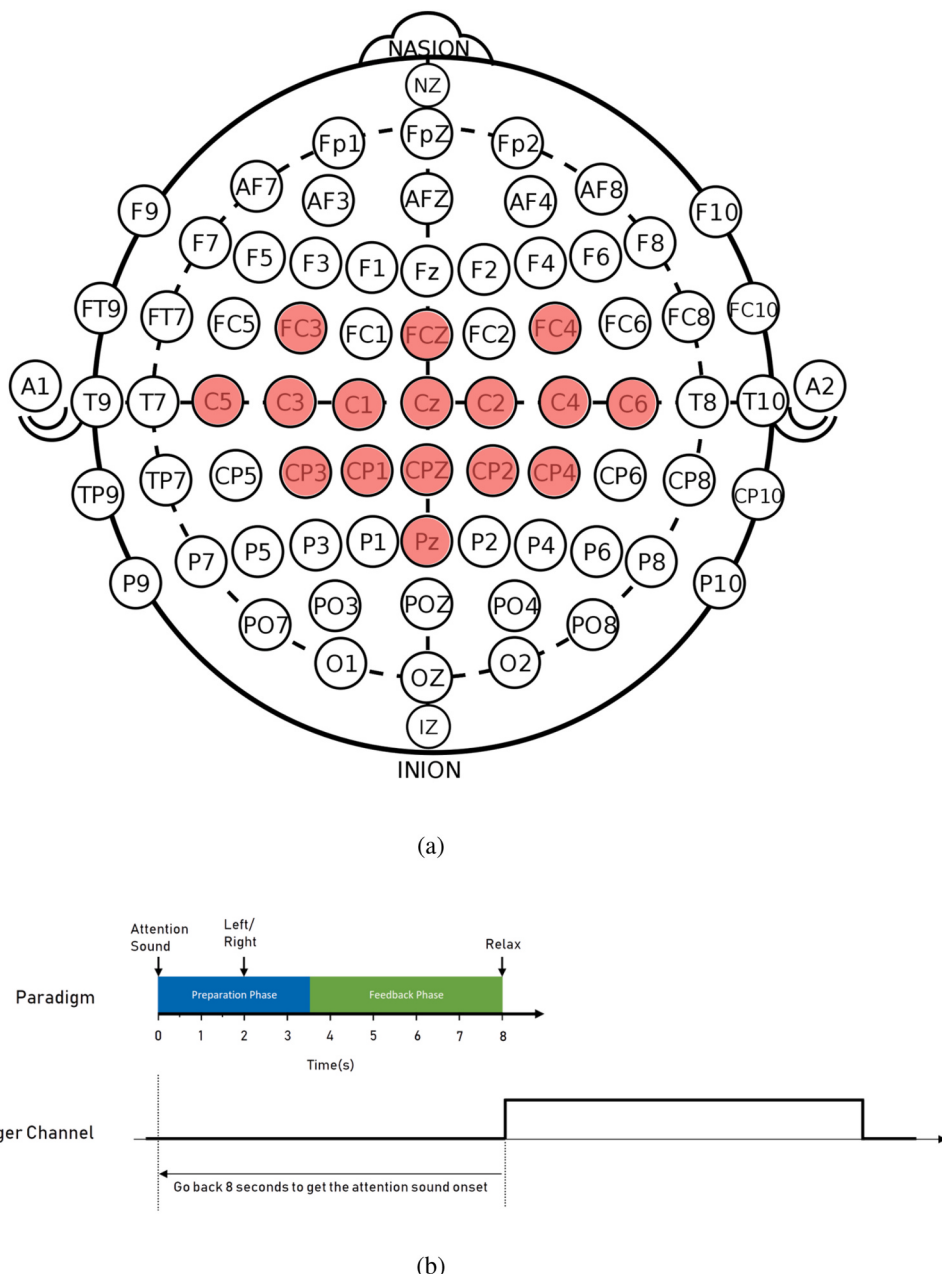


Fig. 2. (a) EEG electrodes distributions based on 10–20 system, (b) Schematic diagram of EEG recording protocol.

automatically assign the changes pre- and post-MI-based BCI rehabilitation performing a mental task. In this section, different classification algorithms were used, namely, support vector machine (*SVM*), *k* nearest neighbours (*kNN*) and Random forest (*RF*).

In this study, the *RBF*-base kernel were utilised for multi-class *SVM* classifiers with the smoothing parameter σ of 0.5 that minimises the misclassification accuracy rate of the training dataset.

The *kNN* scheme is one of the most popular non-parametric classification algorithms and is more robust when $k > 1$, particularly for reducing the influenced noisy points within the training set. In this study, the *Euclidean* distance was utilised as a similarity measure to classify each trial by *kNN*. The classifier was trained to obtain the best value of $k = 7$, which maximises the overall classification performance evaluation.

The *RF* was included in this study in the classification of the feature set for comparison as it belongs to the rule-based family and is regarded as supervised learning. Previous studies have used *RF* for classifying signals [86,87]. *RF* can improve the accuracy of a signal classification by using a voting system to identify the most suitable class. This approach is popular for classifying bioelectrical signals like the EEG and for biomedicine and has proven effective and robust for classification [88].

The classification model parameters for the training and testing datasets were determined via 10-fold cross validation using a grid search approach to avoid overfitting and bias in the classification analysis. In this work, the classification model's labels were classified into pre- and post-rehabilitation. The pre-rehabilitation dataset was labeled as class 1 and the post-rehabilitation dataset was labeled as class 2. Therefore, each of the pre- and post-rehabilitation datasets was divided into 10 equal size disjoint subsets. One of these subsets was used as the test set, and the remaining nine subsets were combined into a training set to learn the classifier. This procedure was performed 10 times and resulted in 10 accuracies. The average of these accuracies represented the 10-fold cross-validation accuracy of learning from this dataset.

The performance of the proposed framework was evaluated using the values of average classification accuracy. The overall average accuracy is computed using the following equation:

$$\text{Accuracy} = \frac{x}{N} \times 100 \quad (23)$$

where x refers to the number of correctly classified input data points and N refers to the total number of attributes.

5. Results and discussions

This section explains the main finding for the proposed method and framework. Section 5.1 provides details of the EEG dataset which are used in this work. Section 5.2 provides the results of the prepossessing stage used in this work. Sections 5.3, 5.4, 5.5 and 5.6 present the outcomes of the time domain, entropy domain frequency domain and fusion features, respectively. The comparison of the results of the proposed method with those of state-of-the-art techniques are explained in Section 5.7. Finally, the discussion of all results are provided in Section 5.8.

5.1. EEG dataset

The EEG dataset from the post-stroke patients with upper extremity hemiparesis was investigated. Three post-stroke patients treated with the recoverIX system (g.tec medical engineering GmbH) were enrolled in this study, participants had a mean age of 22 years ($SD = 4.582$). Each participant received three months of BCI-based MI training with two training sessions per week (for a total of 25 training sessions). Two assessments (pre- and post-training) were performed and were evaluated by the research team. The pre-training assessment was scheduled at 30–35 days before the intervention, and the post-training counterpart was carried out a few days after the intervention (see Fig. 2). This study protocol was approved by the Ethikkommission des Landes Oberösterreich in Austria ($D = 42 - 17$) and each patient signed informed consent before the pre-assessment. Finally, this dataset is recorded with a 256Hz sampling rate.

The patients were asked to imagine dorsal wrist movement according to the system indications of an MI mental task. The patients performed 25 MI-based BCI sessions with follow up assessment visits to examine the functional changes pre- and post- EEG neurorehabilitation. Each session consisted of 240 MI repetitions on both hands divided into three runs of 80 trials. The total duration of each session was approximately 1 h, including the preparation and cleaning period. The MI-based BCI tasks were illustrated in pseudo random order with randomised inter-trial intervals.

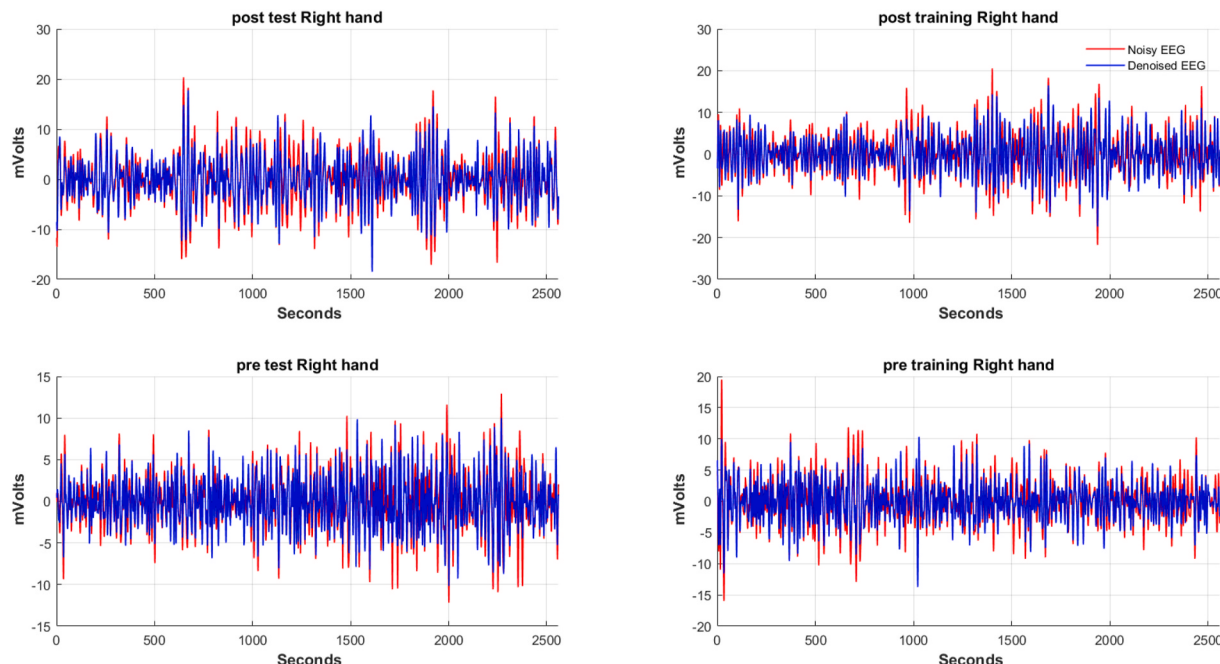


Fig. 3. The filtration results after applying the conventional filters and AICA-WT technique on the EEG channel Ch5 which represent C3.

Table 2

Comparison results of classification accuracy between the conventional filters, AICA, WT and the proposed method (AICA-WT).

Subject	Stage	Purpose	Conventional			AICA-WT			AICA			WT		
			KNN	SVM	RF	KNN	SVM	RF	KNN	SVM	RF	KNN	SVM	RF
P1	Pre	Training	58.5	60.67	64.83	71.66	66.33	94	70.17	63.67	82	52	57.67	56.17
	Post	Test	61.5	66.17	71.67	98.16	93	99	87.67	92.67	95.33	60	60.83	56.33
P2	Pre	Training	56.83	55.83	56.67	99.16	94.83	99.5	70.17	86.17	97.67	51.33	50	52
	Post	Test	58	62.67	66	99	94.33	99.66	79.83	87.17	91	55	52.83	54.83
P3	Pre	Training	56.17	58.83	60.67	97.83	95.33	99.33	81.5	86.17	96.33	51.5	51.17	50.83
	Post	Test	68.67	75.17	75.67	99.5	95.66	99.66	91.17	94.67	97.67	53.67	52.67	52.83

Table 3

Comparison of the time domain feature classification results used for MI-based BCI.

Subject	Stage	Purpose	Feature	Accuracy (%) of		
				kNN	SVM	RF
P1	Pre	Training	HFD	76.66	74.33	80.33
	Post	Test		97.83	98.5	97.5
P2	Pre	Training	HFD	99.5	99.66	99
	Post	Test		99.5	99.66	99.66
P3	Pre	Training	HFD	99	99.5	99
	Post	Test		100	99.83	99.66
P1	Pre	Training	hjAc	93.5	95.66	94.66
	Post	Test		97.33	98.83	98.16
P2	Pre	Training	hjAc	98.16	99	98.33
	Post	Test		97.33	98	96.66
P3	Pre	Training	hjAc	98	97.16	97.5
	Post	Test		98.66	98.33	98.16
P1	Pre	Training	hjComp	59.5	61.66	68.16
	Post	Test		96	97.66	96.5
P2	Pre	Training	hjComp	96.66	95.66	94
	Post	Test		95.83	93.5	97.83
P3	Pre	Training	hjComp	97.16	95.5	96.83
	Post	Test		98	96.83	97.33
P1	Pre	Training	hjMo	73.16	71	78.83
	Post	Test		99.16	99.5	98.83
P2	Pre	Training	hjMo	96	98.16	97
	Post	Test		98.5	98.83	98
P3	Pre	Training	hjMo	97.66	98.16	98.5
	Post	Test		100	99.5	99.83
P1	Pre	Training	Hur	57.66	50.16	60.16
	Post	Test		70.66	71.16	76.83
P2	Pre	Training	Hur	75.16	72.16	79.16
	Post	Test		85.66	81.5	86.83
P3	Pre	Training	Hur	71.66	70.66	80.83
	Post	Test		90.66	91.5	92.83
P1	Pre	Training	Kurt	62.16	61.83	65.16
	Post	Test		72.66	71.66	78.5
P2	Pre	Training	Kurt	85	81	86.66
	Post	Test		87.66	89	90.16
P3	Pre	Training	Kurt	80	85	84.33
	Post	Test		87.66	88	88.33
P1	Pre	Training	Skw	66.83	65.66	65.83
	Post	Test		71.66	70.33	80.33
P2	Pre	Training	Skw	87	82.16	86.66
	Post	Test		90.83	92	92.5
P3	Pre	Training	Skw	78.83	84	83.66
	Post	Test		90.5	88.83	90

EEG caps with 16 active electrodes from g.Nautilus PRO, g.tec medical engineering GmbH, Austria were used. The EEG electrodes were positioned according to the international 10–20 system as follows: (FC5, FC1, FCz, FC2, FC6, C5, C3, C1, Cz, C2, C4, C6, CP5, CP1, CP2, and CP6). A reference electrode was placed on the right earlobe and a ground electrode at FPz (Fig. 2).

5.2. EEG prepossessing results

By using the AICA-WT proposed method, the final denoising results for Channel 5 (*Ch5*) which represents Central Electrode 3 (C3) is shown in Fig. 3. As we can see, compared with the raw EEG (blue colour), the artifacts (red colour) disappeared while the EEG content was well reserved.

Table 2 shows the effects of implementing the AICA-WT approach relative to those with conventional filters. However, the experiment was conducted according to fused features, specifically, *HjAc*, *impe*, and *meanF*. Furthermore, three classifiers are included (*kNN*, *SVM* and *RF*) to provide a more comprehensive evaluation scenario to measure the effects of the proposed denoising technique on the classification performance. The outcomes generally proved significant effects on the classification performance for the three classifiers. Furthermore, the highest results are generated by the *RF* classifier.

5.3. Time domain results

Table 3 shows the results of seven time domain features including *HFD*, *Skw*, *Kurt*, *Hur*, *HjAc*, *HjComp* and *HjMo*. These features have been evaluated using three different classifiers: *SVM*, *kNN* and *RF*. According to the post-test, the performance of the selected classifiers have fluctuated from one feature to another. For the *HFD* feature, *SVM* achieved the best classification accuracies of 98.5%, 99.66% and 99.83% for Persons 1 (P1), 2 (P2) and 3 (P3), respectively. For the *HjAc* feature, *SVM* obtained 98.83% best accuracy for P1 and 98% for P2, and *kNN* achieved 98.66% for P3. For the *HjComp* feature, *SVM* achieved 97.66% for P1, and *RF* obtained 97.83% for P2 and 98% best accuracy for P3. For the *HjMo* feature, *SVM* obtained 99.5% and 98.83% for P1 and P2, respectively. *kNN* achieved 100% for P3. For the *Hur* feature, the *RF* classifier achieved the best accuracy rate overall as 76.83%, 86.83%, and 92.83% for P1, P2 and P3, respectively. For the *Kurt* feature, the *RF* classifier achieved the best accuracy rates for P1 and P2 as 78.5%, 90.16% and 88.33% for P1, P2 and P3, respectively. For *Skw*, *RF* achieved best accuracies equal to 80.33% and 92.5% for P1 and P2, respectively. *kNN* achieved the best accuracy of 90.5% for P3. Fig. 4 shows the results of the time domain features.

5.4. Entropy domain results

Table 4 presents the classification accuracy results using six entropy features of *FuzEn*, *impe*, *MFE_mu*, *RCMFE_mu*, *SampEn* and *TsEn*. Compared to the other five entropy features, the best classification filter performance was achieved using *impe* with the *kNN* classifier compared to the two other classifiers in almost all the stages for the three patients except for P1 pre-training where the *RF* slightly outperforms with only 1.5%. Similarly, the sample entropy with *kNN* classifier produces higher classification performance compared to the two other classifiers in almost all the stages for the three patients except for the P1 pre-training where the *RF* slightly outperforms with less than 1% and the P3 post-test with almost 0.7%. However, the result of the other classifiers fluctuated from one feature to another as shown in Fig. 5.

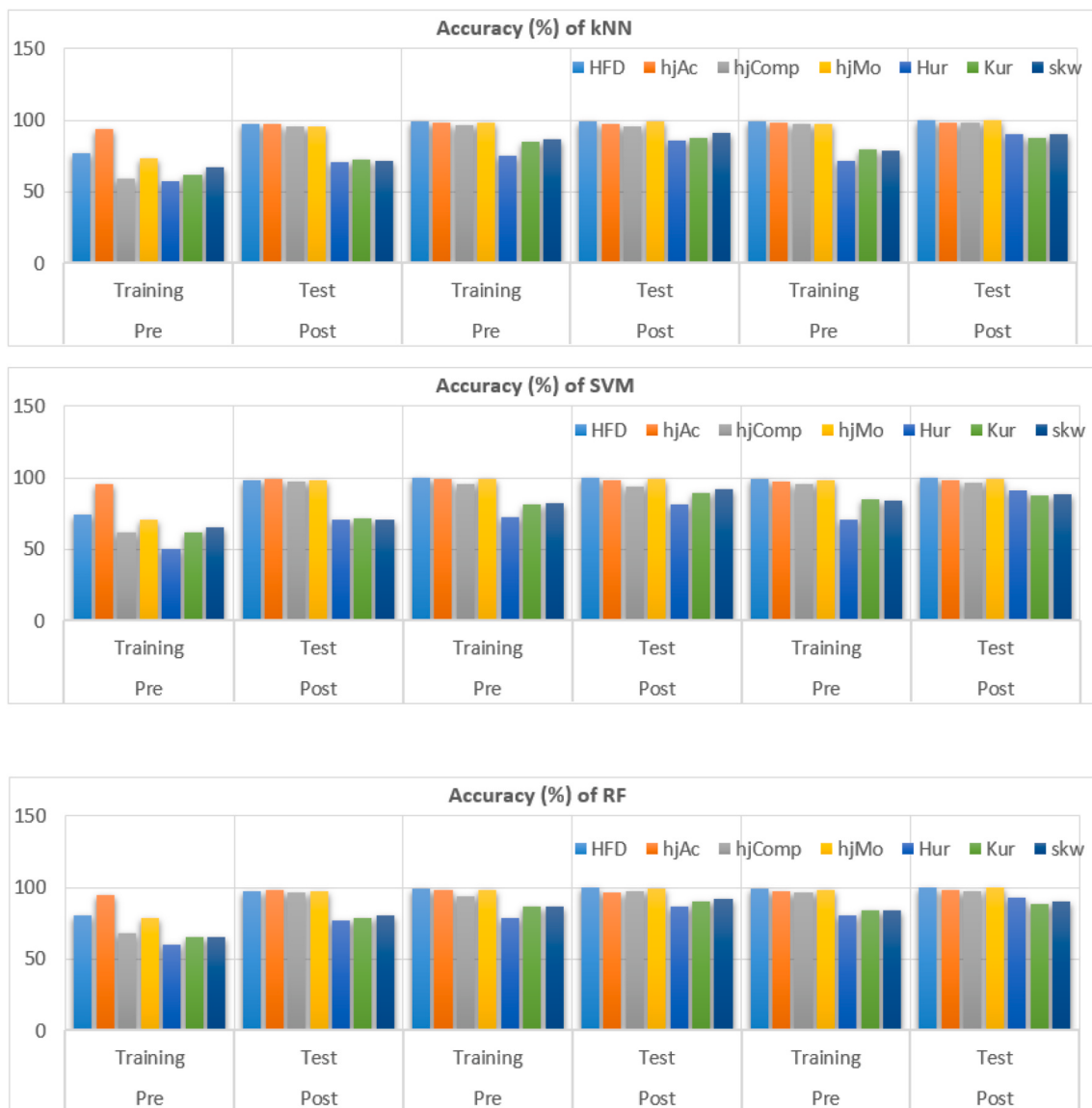


Fig. 4. Comparison of the time domain feature classification results used for MI-based BCI.

5.5. Frequency domain results

Table 5 shows the results of classification according to the two frequency domain features of *meanF* and *medF*. In the training and testing stages, *meanF* showed significant impact relative to the *medF* feature on the overall predication results for the three classifiers. However, SVM showed the dominant performance compared to other classifiers in the training and testing phases within P2 and P3 data according to the *meanF* constraints. Moreover, the kNN and RF have scored adequate and close classification results relative to the SVM. Nevertheless, the RF has showed the leading performance in contrast to other classifiers in terms of the training and testing phases for the three patients' data on the basis of *medF* constraints. In the training phase, SVM has the uppermost performance with a score of 98.83%, and same classifier scored the minimum rate with 65.83%. The highest accuracy result in the testing stage was achieved by kNN with 99.5%, and SVM scored the minimum rate with 67.66% as in Fig. 6.

5.6. Fusion results

Table 6 shows the accuracy results of the proposed TEF fusion feature

set between the subjects for the pre-and post-training stages. The results of the proposed TEF feature set with the RF classifier outperform those of the kNN and SVM classification models. Moreover, the results have higher accuracy values at the post-training stages than at the pre-training stages ($TEF_RF_pre < TEF_RF_post$) for all patients.

Therefore, the TEF feature set has good descriptions and investigations from the three domains in our case towards improving the final classification results particularly for the RF classifier as in Fig. 7.

5.7. Comparison with state-of-the-art methods

The CSP + LDA method which was proposed by [57]. In this study, multi-phase assessments were performed two pre-assessments (Pre1 and Pre2) and three post-assessments (Post1, Post2, and Post3) by two certified physiotherapists and were evaluated by the research team. In the preprocessing, a biosignal amplifier "bandpass filtered" (4th order Butterworth filter) was used between 8 and 30 Hz. Also, a common spatial patterns (CSP) are applied in the feature extraction stage to transform the data to a new matrix with a minimal variance of one class and maximal variance of the other class. In addition, the study classified each trial as either left or right MI by linear discriminant analysis (LDA).

Table 4

Comparison of the entropy domain feature classification results used for MI-based BCI.

Subject	Stage	Purpose	Feature	Accuracy (%) of		
				kNN	SVM	RF
P1	Pre	Training	FuzEn	87.16	84.16	87.66
	Post	Test		96.16	95.16	94
P2	Pre	Training	FuzEn	97.16	95.83	97.33
	Post	Test		97.66	97.16	97.33
P3	Pre	Training	FuzEn	89.33	86.5	92.16
	Post	Test		98	95	97.66
P1	Pre	Training	impe	64.5	60.83	66
	Post	Test		96.66	96.5	96.33
P2	Pre	Training	impe	98.66	92.16	96.83
	Post	Test		98.66	98.5	98.16
P3	Pre	Training	impe	97.83	97	96.5
	Post	Test		98.16	98.16	97.83
P1	Pre	Training	MFE_mu	92.66	88.5	93.16
	Post	Test		95.33	95.66	94.16
P2	Pre	Training	MFE_mu	94.83	93.16	96.16
	Post	Test		95.33	92.5	93
P3	Pre	Training	MFE_mu	95.66	97.16	95.5
	Post	Test		96.16	97.16	95.66
P1	Pre	Training	RCMFE_mu	71.83	67.83	73.83
	Post	Test		94.33	93.33	94.5
P2	Pre	Training	RCMFE_mu	93.66	93	94
	Post	Test		94.83	89.33	93
P3	Pre	Training	RCMFE_mu	90.66	83	91.16
	Post	Test		93.66	95	94.83
P1	Pre	Training	SampEn	68.66	61.83	69.5
	Post	Test		97.83	96.33	97.33
P2	Pre	Training	SampEn	95.66	94.83	94.16
	Post	Test		95.5	89.5	93.5
P3	Pre	Training	SampEn	91.5	78.33	90.33
	Post	Test		97.66	98	98.33
P1	Pre	Training	TsEn	68	62.33	65.66
	Post	Test		77.16	73.5	79.66
P2	Pre	Training	TsEn	87.5	83.83	88
	Post	Test		93.5	93.66	92.5
P3	Pre	Training	TsEn	80	84.33	86.16
	Post	Test		93	90.66	93.83

On the other hand [45], presented a PCA + TVLDA method, a novel classification method for invasive motor-control BCIs that extends LDA to account for time-variant features. The presented method used a notch-filter cascade (recursive 6th-order Butterworth, bandwidth: 5 Hz) up to the 6th harmonic was used to remove interference peaks from the spectrum at integer multiples of the power line frequency. Besides, an optional spectral whitening filter (impulse response filter) was applied to each channel to enable whitening for real-time applications, where time-frequency transformation is not an option. Common spatial patterns (CSPs) are used for dimension reduction in ECoG signal processing. Authors used time-variant linear discriminant analysis (TVLDA) over standard LDA for classification because TVLDA utilizes information of all individually trained LDA classifiers over the whole trial, which makes it inherently time-variant. Then, for reduction feature dimensionality, a novel approach that is intrinsic to TVLDA is conducted based on principal component analysis (PCA). Lastly [44], introduced a Covariance Matrix Adaptation the evolution Strategy (CMA-ES) technique is proposed to automatically optimize Spatial and frequency-selection filters to providing high-quality attributes to the classifier. To improve classification rates for brain-computer interfaces. According to the preliminary experiments, linear classifiers such as Linear Discriminant Analysis (LDA a.k.a. the Fisher Discriminant or FD) and linear-kernel Support Vector Machines (SVM) can be worked better than nonlinear ones for the selected dataset.

A comparison with state-of-the-art methods was conducted to evaluate classification accuracies. The set of TEF-Fusion with the results of

the three classifiers (kNN, SVM and RF) are compared with those of other methods, namely, CSP + LDA in [57] the following details are used bandpass filtered (4th order Butterworth filter) between 8 and 30 Hz, common spatial patterns (CSP), and linear discriminant analysis (LDA) for preprocessing, feature extraction, and classification phase, respectively. PCA + TVLDA in [45] the following details are used Principal component analysis (PCA), and Time-Variant Linear Discriminant Analysis (TVLDA) for feature extraction, and classification phase, respectively. CSP + CMA-ES [44] the following details are used common spatial patterns (CSP), and Covariance Matrix Adaptation Evolution Strategy (CMA-ES). The results of the proposed TEF Fusion registered significant improvement in the average accuracy in the post-analysis for the three-stroke patients' data (see Table 7). For instance, in the post-training phase, the comparison indicated that the TEF-Fusion method has high accuracy with the kNN classifier with respect to P2 (differentiate ratio were 12.9% in [57]; 1.8% in [45]; 23.89% in [44] and P3 (16.6% in [57]; 3.4% in [45]; and 41.74% in [44]). Moreover, the TEF-Fusion classification results with the RF classifier were also higher than those of the state-of-the-art approaches for the P1, P2 and P3 patients. The outcomes for P1 involve 15.1% in [57]; 0.6% in [45]; 21.04% in [44]; for P2 were 13.56% in [57]; 2.46% in [45]; 24.55% in [44]) and respect to P3 (16.76% in [57]; 3.56% in [45]; and 41.9% in [44]). Thus, for the fusion results in the post-analysis, a significant improvement occurs in the average accuracy relative to the classification results from benchmark studies in the literature as shown in Fig. 8.

Note that the AICA-WT-TEF framework can yield useful information to characterise and identify MI changes from BCI-based EEGs. The proposed framework represented by the TEF feature set outperforms other feature sets by improving the classification overall accuracy for all the patients that underwent MI-based BCI rehabilitation. Therefore, the combined TEF features can complement each other towards the best performance that could be achieved by using the AICA-WT-TEF proposed framework.

5.8. Discussions

Prior to actually presenting our findings for the state-of-the-art analysis, we would like to stress that it was not our goal to optimize the overall effectiveness of system, but rather to examine the influence of denoising and feature extraction methodological approaches on the classification accuracy. In other words, we improved the prepossessing stage rather than the classifier model itself. This study adopted an EEG dataset from the public online repository of the g.tec medical engineering GmbH for three post-stroke patients. The topography visualization of brain patterns during MI-based BCI using the proposed method is shown in Fig. 9. The power spectral density (DSP) has been used to represent to show the topography different between before and after proposed method applied.

To further improve the classification performance of the stroke EEG signals', three types of features (namely, time, entropy and frequency domains) were used as the baseline for the classification task. Along with the view of highlighting the most powerful feature, two scenarios were adopted for the classification of stroke EEG signals, for which each scenario examined the same set of classifiers. Thus, the feature that improved the accuracy of selected classifiers can be identified.

First, classification was performed according to the individual feature domain. In the time domain, seven features were tested, and the *HjAc* feature had the most significant influence on the improvement of the classification task especially in the post-testing phase for each of the kNN, SVM, and RF classifiers. Furthermore, the *impe* feature showed momentous impact on the classification results relative to other five features of the entropy domain. The accuracy improvement can be seen especially in the pre-training phase for each of the kNN, SVM, and RF classifiers. However, in testing phase, this feature has low impact, specifically in the kNN classification results. Even with that flaw the classification result based on this feature still can increase the accuracy

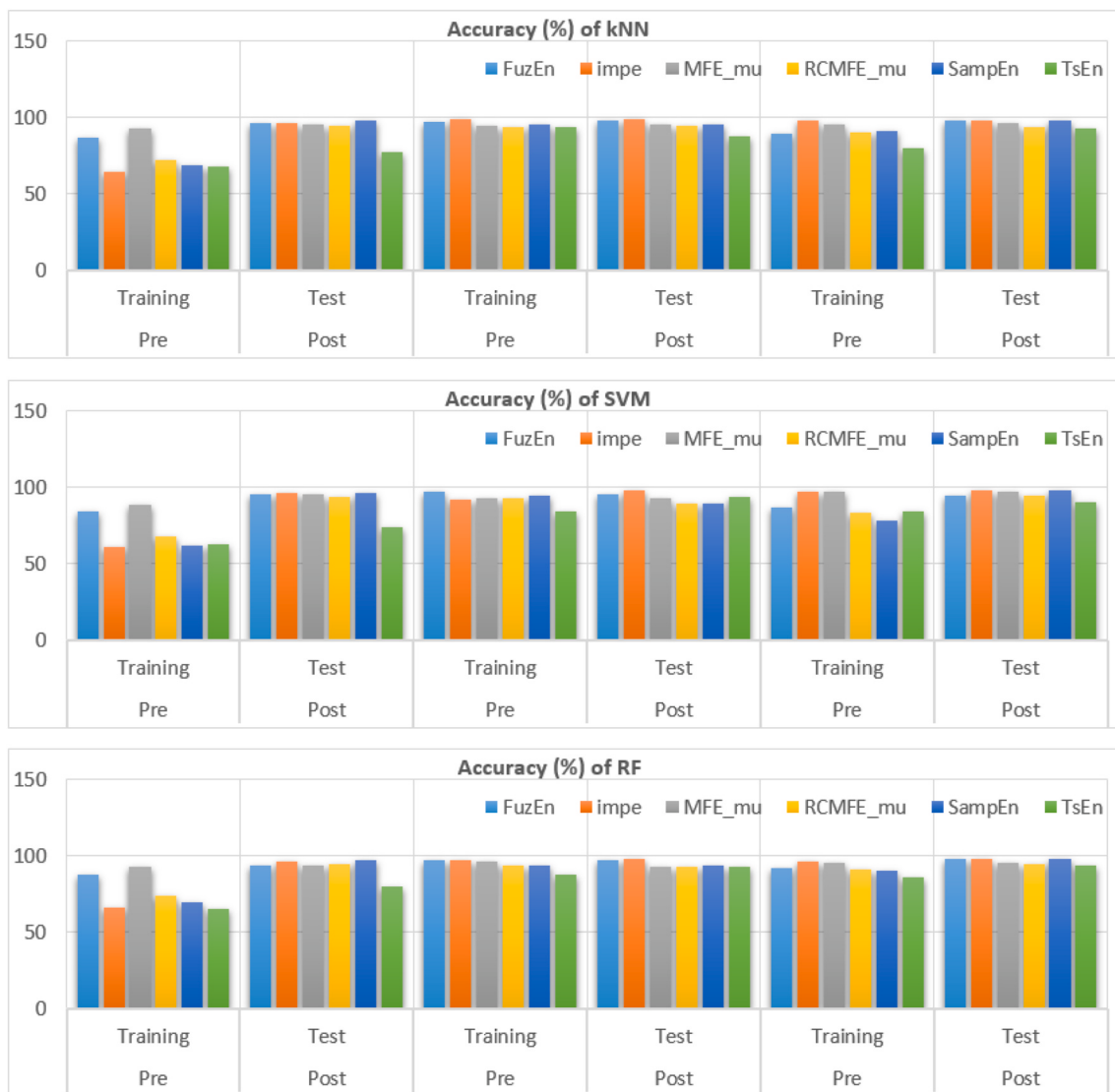


Fig. 5. Comparison of the entropy domain feature classification results used for MI-based BCI.

Table 5

Comparison of the frequency domain feature classification results used for MI-based BCI.

Subject	Stage	Purpose	Feature	Accuracy (%) of		
				kNN	SVM	RF
P1	Pre	Training	meanF	76.5	70.5	78.33
	Post	Test		94.83	96.33	96.5
P2	Pre	Training	medF	97.5	98.83	98
	Post	Test		98.5	99.16	98.33
P3	Pre	Training	meanF	95.66	98	96.66
	Post	Test		99.5	99.16	99.33
P1	Pre	Training	medF	69.83	65.83	74.16
	Post	Test		75.5	67.66	78.5
P2	Pre	Training	meanF	81.33	81.83	88
	Post	Test		85.66	87.16	88.16
P3	Pre	Training	meanF	84.83	84.33	90
	Post	Test		91	87.16	94.16

performance compared with other ones. A low accuracy result was found in the P1 data, particularly in the testing phase, in the most of classification results based on different domains features. This outcome may arise because of the shape of the data. Furthermore, unlike the original BCI data which is recorded on healthy individuals, we used

stroke patients' dataset. However, in the classification results from the frequency domain features, *meanF* showed a salient ameliorating effect in the accuracy for the three classifiers compared with the *medF* feature. Moreover, the outstanding improvement for the classification stage with premise of *meanF* were observed for the training and testing phases.

Second, in the classification stage, the most difficult task involve the nature and the size of the feature, particularly when the dimension of the feature set is too big. According to the previous scenario, this study investigated the effect of the 15 features from three different aspects of views (domains) individually. This approach leads to an extensive feature set that will be examined by the classification models. Therefore, the proposed TEF features fusion set was strongly promoted to combine the most effective and prominent features from each domain and control some of each domain's shortcomings. Performance is thus improved, and lower system complexity is achieved.

According to the classification results on the basis of the features from three different domains types, three features exerted significant impacts on the classification performance, and these include *HjAc*, *impe* and *meanF*. These three features were used as the cornerstone for the classification task based on the fusion of extracted features. According to the fusion results in both pre- and post-analyses, a significant improvement occurred in the average accuracy relative to the classification result on the basis of the individual feature domain. For instance,

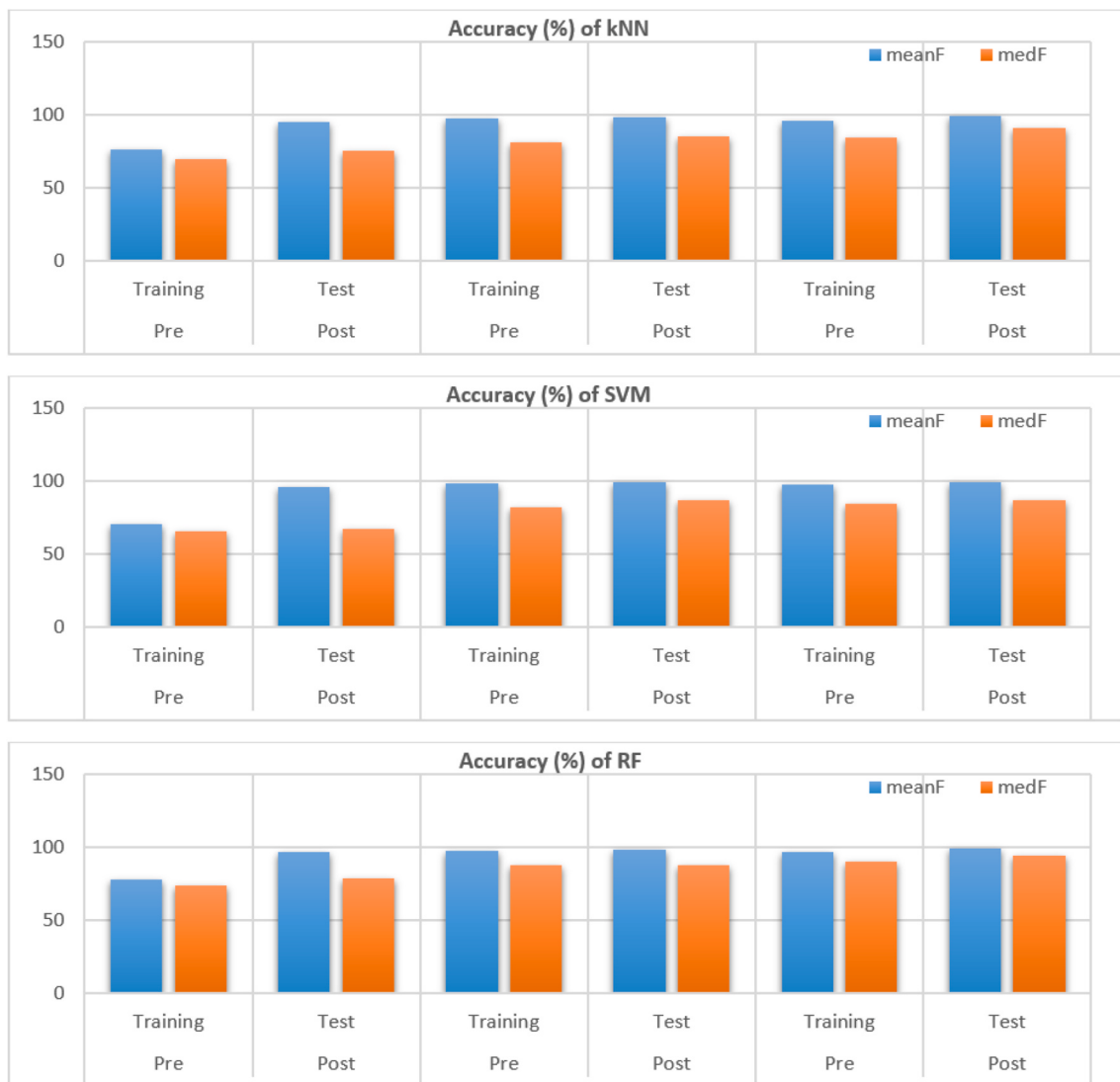


Fig. 6. Comparison of the frequency domain feature classification results used for MI-based BCI.

Table 6
Comparison of the fusion feature classification results used for MI-based BCI.

Subject	Stage	Purpose	Accuracy (%) of		
			kNN	SVM	RF
P1	Pre	Training	71.66	66.33	94
	Post	Test	98.16	93	99
P2	Pre	Training	99.16	94.83	99.5
	Post	Test	99	94.3333	99.66
P3	Pre	Training	97.83	95.33	99.33
	Post	Test	99.5	95.66	99.66

in the pre-training phase, the average accuracy based only on the *meanF* feature is 90.99% in kNN, and the result of the same classifier on the basis of the fusion of the three features is 97.61%. Consequently, the improvement rate reached 6.6%. By contrast, the testing (post) phase showed classification result using the *impe* feature as 97.44% in SVM, and the result using fusion is 99.44%, with a 2% accuracy improvement rate. However, the highest accuracy improvement was achieved in the post analysis results for the RF classifier with 11.16%. The average accuracy for this classifier based on the *impe* feature is 86.44%, and the fusion results is 97.61%. This outcome was followed by 6.61% as the improvement rate for the same classifier in the training phase with

meanF constraints. In general, the fused features have more noticeable impact on the training in the post phase. The fusion process has also showed a great impact on the accuracy improvement for almost all classifiers with the *impe* feature. However, the enhancement rate for some classifiers is varied for each of *HjAc* and *meanF* features. Nevertheless, several limitations also need to be considered, including the finding that the proposed framework relied on the set of features from multiple domains. Moreover, the sample size was small and further investigations with a larger database is needed in future research. This work undertook a comparison of the time, entropy and frequency feature sets and an integrated *TEF* feature set. The features used are worth investigating to determine their potential for MI-based investigation on EEG signals. Nevertheless, the suggested EEG-based method does have a limitation, as this study did not employ a control group, thereby limiting direct comparisons between the approach used herein and conventional techniques. The effectiveness of BCI therapy over conventional therapy was already demonstrated in several publications using other approaches [44,45,57] as shown in the comparison of state-of-the-art techniques in 7.

The objective of this investigation was also to explore the effects of the approach used here to assess whether results are similar to those of other studies and whether they have clinical value. In addition, not all patients could perform all the test pre- and post-rehabilitation therapy.

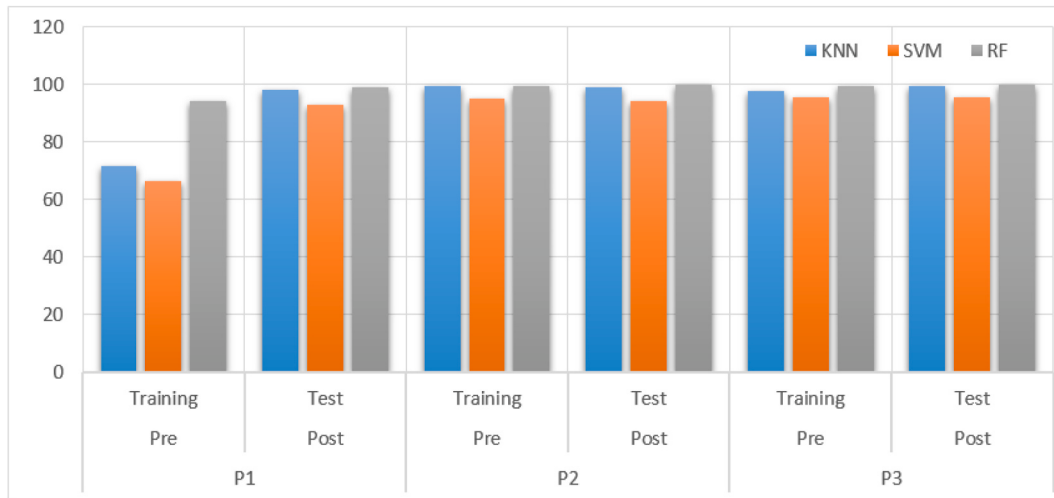


Fig. 7. Comparison of the fusion feature classification results used for MI-based BCI.

Table 7
Comparison results of the proposed method with the state-of-the-art.

Subject	Proposed method			State-of-the-art		
	TEF + kNN	TEF + SVM	TEF + RF	CSP + LDA	PCA + TVLDA	CSP + CMA + ES
P1	98.16	93	99	83.9	98.4	77.96
P2	99	94.3333	99.66	86.1	97.2	75.11
P3	99.5	95.66	99.66	82.9	96.1	57.76

These limitations notwithstanding, an agreement occurs between the results reported by this work and those of other studies, and this outcome confirms the ability of EEG signals to detect the MI changes pre- and post-rehabilitation [44,45,57].

6. Conclusions and future work

Characterizing and extracting features from the MI-based BCI rehabilitation for stroke patients is a global challenge for supporting personalized healthcare. A fusion feature extraction method is applied to select the most important features to obtain a significant improvement in the average accuracy. The TEF fusion method results registered a significant average accuracy improvement compared with the

classification results in the individual feature domain in the post-analyses. For instance, in the pre-training phase, the average accuracy based only on the meanF of the feature is 90 : 99% in KNN, and the result of the same classifier based on the fusion of three features is 97 : 61%. Thus, the improvement rate reached 6 : 6%. By contrast, the testing (post) phase obtained classification results based on impe feature of 97 : 44% in SVM, and the results based on fusion is 99 : 44%, with a 2% accuracy improvement rate (see Discussion Section). Therefore, the fused features have a more noticeable impact on the training than the post phase. A TEF-Fusion attained significant improvement in the average accuracy compared with the classification results based on previous studies in stroke rehabilitation applications in post-analysis with KNN and RF classifiers. For instance, the proposed TEF method registered high scored accuracy improvement with the RF classifier for P3, and the diff tiate ratio compared with the literature was 16.76% in [57]; 3.56% in [45]; and 41.9% in [44] (Table 7). Comparison of the TEF-Fusion method shows high accuracy from the literature with the kNN classifier for P2 and P3. Comparison results for P2 indicated a differentiate ratio of 12.9% in [57]; 1.8% in [45]; 23.89% in [44]. Therefore, the RF classifier achieves the best results compared to other classifiers (SVM and kNN). The proposed TEF method also registered significant performance accuracy measures compared to the state-of-the-art approaches. AICA-WT-TEF framework can yield useful information to characterise and identify MI changes from BCI-based

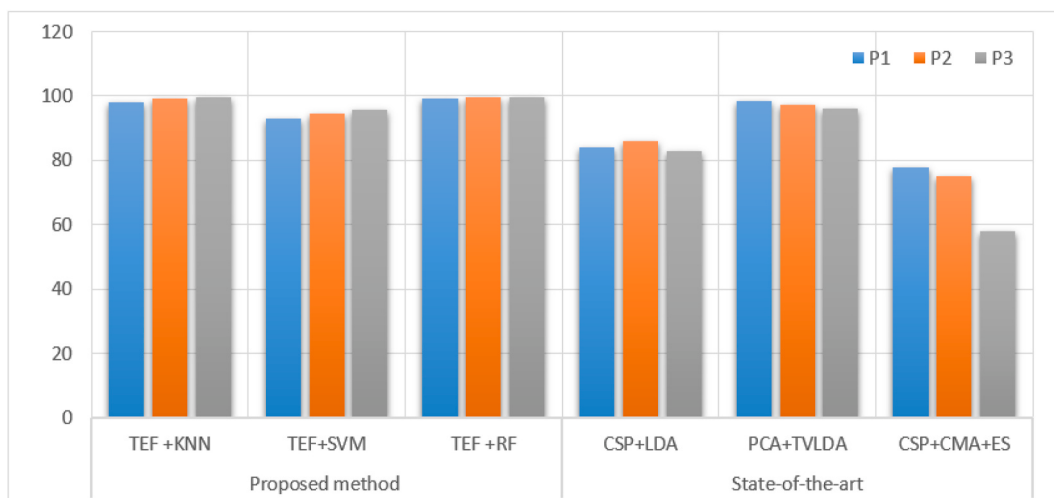


Fig. 8. Comparison of the proposed method with the state-of-the-art.

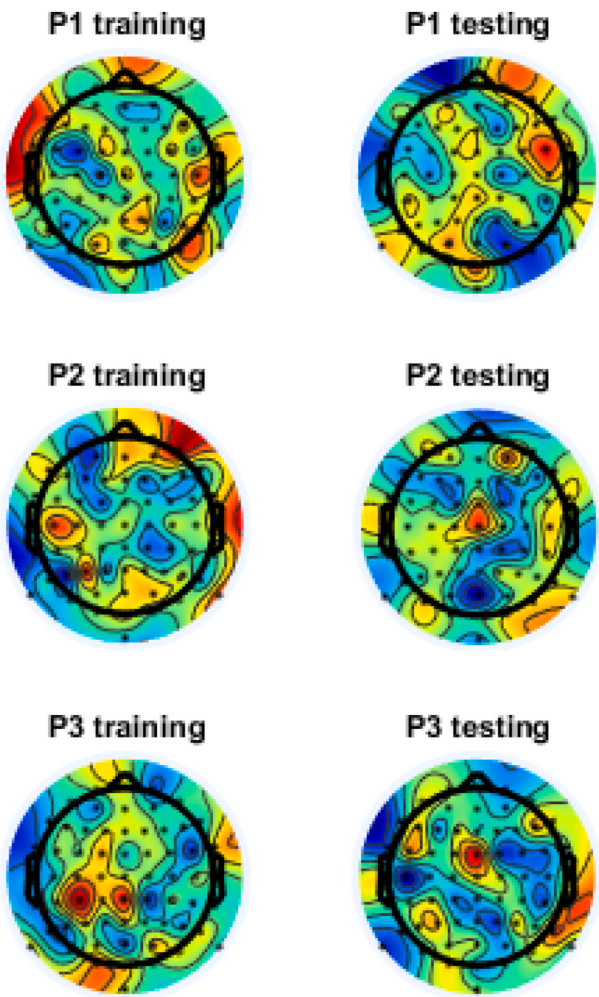


Fig. 9. Topology plot of the proposed method.

EEGs.

For future work, the proposed method will be used with different feature selection approaches, such as that of [89,90]; and for investigating other feature combinations according to various domains. Moreover, the proposed method will be tested in the future through further investigations with a larger database. Another recommended direction is to perform stroke patient rehabilitation to select the best task that can provide the highest accuracy rate. Subsequently, the channel selection method could be applied as in [91,92].

Declaration of competing interest

The authors declare that they have no known competing financial interests or personal relationships that could have appeared to influence the work reported in this paper.

References

- [1] U.R. Acharya, H. Fujita, V.K. Sudarshan, S. Bhat, J.E. Koh, Application of entropies for automated diagnosis of epilepsy using EEG signals: a review, *Knowl. Base Syst.* 88 (2015) 85–96.
- [2] S. Aggarwal, N. Chugh, Signal processing techniques for motor imagery brain computer interface: a review, *Array* 1 (2019) 100003.
- [3] N.K. Al-Qazzaz, S. Hamid Bin Mohd Ali, S. Ahmad, M. Islam, J. Escudero, Automatic artifact removal in EEG of normal and demented individuals using ica-wt during working memory tasks, *Sensors* 17 (2017) 1326.
- [4] N.K. Al-Qazzaz, S. Ali, M.S. Islam, S.A. Ahmad, J. Escudero, EEG markers for early detection and characterization of vascular dementia during working memory tasks, in: 2016 IEEE EMBS Conference on Biomedical Engineering and Sciences (IECBES), IEEE, 2016, pp. 347–351.
- [5] N.K. Al-Qazzaz, S.H.B. Ali, S.A. Ahmad, K. Chellappan, M. Islam, J. Escudero, Role of EEG as biomarker in the early detection and classification of dementia, *The Scientific World Journal* 2014 (2014) 1–17, 2014.
- [6] N.K. Al-Qazzaz, S.H.B.M. Ali, S.A. Ahmad, J. Escudero, Optimal EEG channel selection for vascular dementia identification using improved binary gravitation search algorithm, in: International Conference for Innovation in Biomedical Engineering and Life Sciences, Springer, 2017, pp. 125–130.
- [7] N.K. Al-Qazzaz, S.H.B.M. Ali, S.A. Ahmad, M.S. Islam, J. Escudero, Discrimination of stroke-related mild cognitive impairment and vascular dementia using EEG signal analysis, *Med. Biol. Eng. Comput.* (2017) 1–21.
- [8] N.K. Al-Qazzaz, S.H.B.M. Ali, S.A. Ahmad, M.S. Islam, J. Escudero, Comparison of the effectiveness of aica-wt technique in discriminating vascular dementia EEGs, in: 2018 2nd International Conference on BioSignal Analysis, Processing and Systems (ICBAPS), IEEE, 2018, pp. 109–112.
- [9] N.K. Al-Qazzaz, S.H.B.M. Ali, S.A. Ahmad, EEG wavelet spectral analysis during a working memory tasks in stroke-related mild cognitive impairment patients, in: International Conference for Innovation in Biomedical Engineering and Life Sciences, Springer, 2015, pp. 82–85.
- [10] N.K. Al-Qazzaz, S.H.B.M. Ali, S. Islam, S. Ahmad, J. Escudero, Selection of mother wavelet functions for multi-channel eeg signal analysis during a working memory task, *Sensors* 15 (2015) 29015–29035.
- [11] R. Aler, I.M. Galván, J.M. Valls, Evolving spatial and frequency selection filters for brain-computer interfaces, in: IEEE Congress on Evolutionary Computation, IEEE, 2010, pp. 1–7.
- [12] G. Altan, Y. Kutlu, N. Allahverdi, Deep belief networks based brain activity classification using EEG from slow cortical potentials in stroke, *International Journal of Applied Mathematics, Electronics and Computers* 4 (2016) 205–210.
- [13] Z.A.A. Alyasseri, A.K. Abasi, M.A. Al-Betar, S.N. Makhadmeh, J.P. Papa, S. Abdullah, A.T. Khader, Eeg-based person identification using multi-verse optimizer as unsupervised clustering techniques, *Evolutionary Data Clustering: Algorithms and Applications* 89 (2021).
- [14] Z.A.A. Alyasseri, A.T. Khader, M.A. Al-Betar, O.A. Alomari, Person Identification Using EEG Channel Selection with Hybrid Flower Pollination Algorithm, *Pattern Recognition*, 2020, p. 107393.
- [15] Z.A.A. Alyasseri, A.T. Khader, M.A. Al-Betar, J.P. Papa, O.A. Alomari, EEG feature extraction for person identification using wavelet decomposition and multi-objective flower pollination algorithm, *Ieee Access* 6 (2018) 76007–76024.
- [16] H.U. Amin, A.S. Malik, R.F. Ahmad, N. Badruddin, N. Kamel, M. Hussain, W.T. Chooi, Feature extraction and classification for EEG signals using wavelet transform and machine learning techniques, *Australasian physical & engineering sciences in medicine* 38 (2015) 139–149.
- [17] K.K. Ang, C. Guan, K.S.G. Chua, B.T. Ang, C.W.K. Kuah, C. Wang, K.S. Phua, Z.Y. Chin, H. Zhang, A large clinical study on the ability of stroke patients to use an EEG-based motor imagery brain-computer interface, *Clin. EEG Neurosci.* 42 (2011) 253–258.
- [18] H. Azami, J. Escudero, Improved multiscale permutation entropy for biomedical signal analysis: interpretation and application to electroencephalogram recordings, *Biomed. Signal Process Contr.* 23 (2016) 28–41.
- [19] H. Azami, A. Fernández, J. Escudero, Refined multiscale fuzzy entropy based on standard deviation for biomedical signal analysis, *Med. Biol. Eng. Comput.* 55 (2017) 2037–2052.
- [20] H. Azami, S. Sanei, Spike detection approaches for noisy neuronal data: assessment and comparison, *Neurocomputing* 133 (2014) 491–506.
- [21] G. Barbati, C. Porcaro, F. Zappasodi, P.M. Rossini, F. Tecchio, Optimization of an independent component analysis approach for artifact identification and removal in magnetoencephalographic signals, *Clin. Neurophysiol.* 115 (2004) 1220–1232.
- [22] C. Bentes, A.R. Peralta, P. Viana, H. Martins, C. Morgado, C. Casimiro, A.C. Franco, A.C. Fonseca, R. Geraldes, P. Canhão, et al., Quantitative EEG and functional outcome following acute ischemic stroke, *Clin. Neurophysiol.* 129 (2018) 1680–1687.
- [23] A.M. Bhatti, M. Majid, S.M. Anwar, B. Khan, Human emotion recognition and analysis in response to audio music using brain signals, *Comput. Hum. Behav.* 65 (2016) 267–275.
- [24] T.W. Boonstra, S. Nikolin, A.C. Meisner, D.M. Martin, C.K. Loo, Change in mean frequency of resting-state electroencephalography after transcranial direct current stimulation, *Front. Hum. Neurosci.* 10 (2016) 270.
- [25] T.W. Boonstra, S. Nikolin, A.C. Meisner, D.M. Martin, C.K. Loo, Change in mean frequency of resting-state electroencephalography after transcranial direct current stimulation, *Front. Hum. Neurosci.* 10 (2016) 270.
- [26] L. Breiman, Random forests, *Mach. Learn.* 45 (2001) 5–32.
- [27] H. Cai, Z. Qu, Z. Li, Y. Zhang, X. Hu, B. Hu, Feature-level fusion approaches based on multimodal eeg data for depression recognition, *Inf. Fusion* 59 (2020) 127–138.
- [28] R.I. Carino-Escobar, P. Carrillo-Mora, R. Valdés-Cristerna, M.A. Rodríguez-Barragán, C. Hernández-Arenas, J. Quinzáos-Fresnedo, M.A. Galicia-Alvarado, J. Cantillo-Negrete, Longitudinal analysis of stroke patients' brain rhythms during an intervention with a brain-computer interface, *Neural Plast.* 2019 (2019) 1–12, 2019.
- [29] J. Carr, R. Shepherd, Clinical physiotherapy specialisation in Australia: some current views, *Aust. J. Physiother.* 42 (1996) 9–14.
- [30] O. Carrera-León, J.M. Ramírez, V. Alarcon-Aquino, M. Baker, D. D'Croz-Baron, P. Gomez-Gil, A motor imagery bci experiment using wavelet analysis and spatial patterns feature extraction, in: 2012 Workshop on Engineering Applications, IEEE, 2012, pp. 1–6.
- [31] N.P. Castellanos, V.A. Makarov, Recovering EEG brain signals: artifact suppression with wavelet enhanced independent component analysis, *J. Neurosci. Methods* 158 (2006) 300–312.

- [34] T.P. Chou, W.R. Wang, T.S. Chang, Low complexity real time bci for stroke rehabilitation, in: 2015 IEEE International Conference on Digital Signal Processing (DSP), IEEE, 2015, pp. 809–812.
- [35] J. Cillessen, A. Van Huffelen, L. Kappelle, A. Algra, J. Van Gijn, Electroencephalography improves the prediction of functional outcome in the acute stage of cerebral ischemia, *Stroke* 25 (1994) 1968–1972.
- [36] A. Clerico, A. Tiwari, R. Gupta, S. Jayaraman, T.H. Falk, Electroencephalography amplitude modulation analysis for automated affective tagging of music video clips, *Front. Comput. Neurosci.* 11 (2018) 115.
- [37] A. Colomer Granero, F. Fuentes-Hurtado, V. Naranjo Orredo, J. Guixeres Provinciale, J.M. Ausín, M. Alcañiz Raya, A comparison of physiological signal analysis techniques and classifiers for automatic emotional evaluation of audiovisual contents, *Front. Comput. Neurosci.* 10 (2016) 74.
- [38] E.C. Djamal, D.P. Gustiawan, D. Djajasasmita, Significant variables extraction of post-stroke EEG signal using wavelet and som kohonen, *Telkomnika* 17 (2019).
- [39] E.C. Djamal, R.I. Ramadhan, M.I. Mandasari, D. Djajasasmita, Identification of post-stroke EEG signal using wavelet and convolutional neural networks, *Bulletin of Electrical Engineering and Informatics* 9 (2020) 1890–1898.
- [40] B.H. Dobkin, Rehabilitation after stroke, *N. Engl. J. Med.* 352 (2005) 1677–1684.
- [41] J. Escudero, R. Hornero, D. Abásolo, A. Fernández, Quantitative evaluation of artifact removal in real magnetoencephalogram signals with blind source separation, *Ann. Biomed. Eng.* 39 (2011) 2274–2286.
- [42] J. Escudero, R. Hornero, D. Abásolo, A. Fernández, Blind source separation to enhance spectral and non-linear features of magnetoencephalogram recordings. application to alzheimer's disease, *Med. Eng. Phys.* 31 (2009) 872–879.
- [43] B. Foreman, J. Claassen, Quantitative EEG for the detection of brain ischemia, in: Annual Update in Intensive Care and Emergency Medicine 2012, Springer, 2012, pp. 746–758.
- [44] M. Gottlibke, O. Rosen, B. Weller, A. Mahagney, N. Omar, A. Khuri, I. Srugo, J. Genizi, Stroke identification using a portable EEG device—a pilot study, *Neurophysiol. Clin.* 50 (2020) 21–25.
- [45] C. Grefkes, G.R. Fink, Connectivity-based approaches in stroke and recovery of function, *Lancet Neurol.* 13 (2014) 206–216.
- [46] J. Gruenwald, A. Znobishchev, C. Kapeller, K. Kamada, J. Schäringer, C. Guger, Time-variant linear discriminant analysis improves hand gesture and finger movement decoding for invasive brain-computer interfaces, *Front. Neurosci.* 13 (2019) 901.
- [47] H. Gürüler, A novel diagnosis system for Parkinson's disease using complex-valued artificial neural network with k-means clustering feature weighting method, *Neural Comput. Appl.* 28 (2017) 1657–1666.
- [48] M.M. Hassan, M.G.R. Alam, M.Z. Uddin, S. Huda, A. Almogren, G. Fortino, Human emotion recognition using deep belief network architecture, *Inf. Fusion* 51 (2019) 10–18.
- [49] G. Henderson, E. Ifeachor, N. Hudson, C. Goh, N. Outram, S. Wimalaratna, C. Del Percio, F. Vecchio, Development and assessment of methods for detecting dementia using the human electroencephalogram, *Biomedical Engineering, IEEE Transactions on* 53 (2006) 1557–1568.
- [50] R. Hornero, J. Escudero, A. Fernández, J. Poza, C. Gómez, Spectral and nonlinear analyses of MEG background activity in patients with alzheimer's disease, *IEEE (Inst. Electr. Electron. Eng.) Trans. Biomed. Eng.* 55 (2008) 1658–1665.
- [51] A. Hyvärinen, Fast and robust fixed-point algorithms for independent component analysis, *Neural Networks, IEEE Transactions on* 10 (1999) 626–634.
- [52] Z. Iscan, Z. Dokur, T. Demirpal, Classification of electroencephalogram signals with combined time and frequency features, *Expert Syst. Appl.* 38 (2011) 10499–10505.
- [53] C.J. James, C.W. Hesse, Independent component analysis for biomedical signals, *Physiol. Meas.* 26 (2005) R15.
- [54] R. Jenke, A. Peer, M. Buss, Feature extraction and selection for emotion recognition from EEG, *IEEE Transactions on Affective computing* 5 (2014) 327–339.
- [55] V.J. Kartsch, S. Benatti, P.D. Schiavone, D. Rossi, L. Benini, A sensor fusion approach for drowsiness detection in wearable ultra-low-power systems, *Inf. Fusion* 43 (2018) 66–76.
- [56] W. Khairunizam, C.W. Yean, M. Murugappan, A.K. Junoh, Z.M. Razlan, A. Shahriman, W.A.W. Mustafa, Z. Ibrahim, S. Nurhafizah, An experimental framework for assessing emotions of stroke patients using electroencephalogram (EEG), in: *Journal of Physics: Conference Series*, IOP Publishing, 2020, 052072.
- [57] S. Khatun, R. Mahajan, B.I. Morshed, Comparative study of wavelet-based unsupervised ocular artifact removal techniques for single-channel eeg data, *IEEE journal of translational engineering in health and medicine* 4 (2016) 1–8.
- [58] A. Khosla, P. Khandnor, T. Chand, A comparative analysis of signal processing and classification methods for different applications based on EEG signals, *Biocybernetics and Biomedical Engineering* 40 (2) (2020) 649–690.
- [59] Y.J. Kim, N.S. Kwak, S.W. Lee, Classification of motor imagery for ear-eeg based brain-computer interface, in: 2018 6th International Conference on Brain-Computer Interface (BCI), IEEE, 2018, pp. 1–2.
- [60] M. Kirkove, C. François, J. Verly, Comparative evaluation of existing and new methods for correcting ocular artifacts in electroencephalographic recordings, *Signal Process.* 98 (2014) 102–120.
- [61] S. Kumar, A. Sharma, K. Mamun, T. Tsunoda, A deep learning approach for motor imagery eeg signal classification, in: 2016 3rd Asia-Pacific World Congress on Computer Science and Engineering (APWC on CSE), IEEE, 2016, pp. 34–39.
- [62] S. Kumar, M. Yadava, P.P. Roy, Fusion of EEG response and sentiment analysis of products review to predict customer satisfaction, *Inf. Fusion* 52 (2019) 41–52.
- [63] C. Li, T. Jia, Q. Xu, L. Ji, Y. Pan, Brain-computer interface channel-selection strategy based on analysis of event-related desynchronization topography in stroke patients, *Journal of healthcare engineering* (2019) 2019.
- [64] F. Li, Y. Fan, X. Zhang, C. Wang, F. Hu, W. Jia, H. Hui, Multi-feature fusion method based on EEG signal and its application in stroke classification, *J. Med. Syst.* 44 (2020) 39.
- [65] A. Liaw, M. Wiener, Classification and regression by randomforest, *R. News* 2 (2002) 18–22.
- [66] R. Liu, Z. Zhang, F. Duan, X. Zhou, Z. Meng, Identification of anisomeric motor imagery eeg signals based on complex algorithms, *Comput. Intell. Neurosci.* (2017) 2017.
- [67] Y. Liu, O. Sourina, M.K. Nguyen, Real-time EEG-based emotion recognition and its applications, in: *Transactions on Computational Science XII*, Springer, 2011, pp. 256–277.
- [68] F. Lotte, M. Congedo, A. Lécuyer, F. Lamarche, B. Arnaldi, A review of classification algorithms for eeg-based brain–computer interfaces, *J. Neural. Eng.* 4 (2007) R1.
- [69] R. Mahajan, B.I. Morshed, Unsupervised eye blink artifact denoising of eeg data with modified multiscale sample entropy, kurtosis, and wavelet-ica, *IEEE Journal of Biomedical and Health Informatics* 19 (2014) 158–165.
- [70] I. Majidov, T. Whangbo, Efficient classification of motor imagery electroencephalography signals using deep learning methods, *Sensors* 19 (2019) 1736.
- [71] N. Mammone, F. La Foresta, F.C. Morabito, Automatic artifact rejection from multichannel scalp EEG by wavelet ICA, *IEEE Sensor. J.* 12 (2011) 533–542.
- [72] E.A. Mohamed, M.Z.B. Yusoff, N.K. Selman, A.S. Malik, Enhancing EEG signals in brain computer interface using wavelet transform, *International Journal of Information and Electronics Engineering* 4 (2014) 234.
- [73] F.C. Morabito, D. Labate, F. La Foresta, A. Bramanti, G. Morabito, I. Palamara, Multivariate multi-scale permutation entropy for complexity analysis of alzheimer's disease EEG, *Entropy* 14 (2012) 1186–1202.
- [74] D. Moretti, G. Frisoni, C. Fracassi, M. Pievani, C. Geroldi, G. Binetti, P. Rossini, O. Zanetti, Mci patients' EEGs show group differences between those who progress and those who do not progress to ad, *Neurobiol. Aging* 32 (2011) 563–571.
- [75] D. Moretti, C. Miniuissi, G. Frisoni, O. Zanetti, G. Binetti, C. Geroldi, S. Galluzzi, P. Rossini, Vascular damage and EEG markers in subjects with mild cognitive impairment, *Clinical neurophysiology* 118 (2007) 1866–1876.
- [76] D. Moretti, O. Zanetti, G. Binetti, G. Frisoni, Quantitative EEG markers in mild cognitive impairment: degenerative versus vascular brain impairment, *Int. J. Alzheimer's Dis.* (2012) 2012.
- [77] K. Natarajan, R. Acharya, F. Alias, T. Tiboleng, S.K. Puthuserry, Nonlinear analysis of EEG signals at different mental states, *Biomed. Eng. Online* 3 (2004) 7.
- [78] U. Orhan, M. Hekim, M. Ozer, EEG signals classification using the k-means clustering and a multilayer perceptron neural network model, *Expert Syst. Appl.* 38 (2011) 13475–13481.
- [79] E.S. Pane, M.A. Hendrawan, A.D. Wibawa, M.H. Purnomo, Identifying rules for electroencephalograph (EEG) emotion recognition and classification, in: 2017 5th International Conference on Instrumentation, Communications, Information Technology, and Biomedical Engineering (ICICI-BME), IEEE, 2017, pp. 167–172.
- [80] T.T. Pham, R.J. Croft, P.J. Cadusch, R.J. Barry, A test of four EOG correction methods using an improved validation technique, *Int. J. Psychophysiol.* 79 (2011) 203–210.
- [81] J.S. Richman, J.R. Moorman, Physiological time-series analysis using approximate entropy and sample entropy, *Am. J. Physiol. Heart Circ. Physiol.* 278 (2000) H2039–H2049.
- [82] M. Sebastián-Romagosa, W. Cho, R. Ortner, N. Murovec, T. Von Oertzen, K. Kamada, B.Z. Allison, C. Guger, Brain computer interface treatment for motor rehabilitation of upper extremity of stroke patients—a feasibility study, *Front. Neurosci.* (2020).
- [83] D. Shon, K. Im, J.H. Park, D.S. Lim, B. Jang, J.M. Kim, Emotional stress state detection using genetic algorithm-based feature selection on EEG signals, *Int. J. Environ. Res. Publ. Health* 15 (11) (2018) 1–11.
- [84] X. Shu, S. Chen, L. Yao, X. Sheng, D. Zhang, N. Jiang, J. Jia, X. Zhu, Fast recognition of bci-inefficient users using physiological features from eeg signals: a screening study of stroke patients, *Front. Neurosci.* 12 (2018) 93.
- [85] L. Sun, et al., Classification of imagery motor eeg data with wavelet denoising and features selection, in: 2016 International Conference on Wavelet Analysis and Pattern Recognition (ICWAPR), IEEE, 2016, pp. 184–188.
- [86] C. Tsallis, Possible generalization of Boltzmann-gibbs statistics, *J. Stat. Phys.* 52 (1988) 479–487.
- [87] E.D. Übeyli, Combined neural network model employing wavelet coefficients for EEG signals classification, *Digit. Signal Process.* 19 (2009) 297–308.
- [88] R. Vigario, E. Oja, Bss and ICA in neuroinformatics: from current practices to open challenges, *IEEE reviews in biomedical engineering* 1 (2008) 50–61.
- [89] J. Xiang, C. Li, H. Li, R. Cao, B. Wang, X. Han, J. Chen, The detection of epileptic seizure signals based on fuzzy entropy, *J. Neurosci. Methods* 243 (2015) 18–25.
- [90] J. Yang, S. Yao, J. Wang, Deep fusion feature learning network for mi-eeg classification, *IEEE Access* 6 (2018) 79050–79059.
- [91] J. Zhou, J. Yao, J. Deng, J.P. Dewald, EEG-based classification for elbow versus shoulder torque intentions involving stroke subjects, *Comput. Biol. Med.* 39 (2009) 443–452.
- [92] X. Zou, M. Lei, Pattern recognition of surface electromyography signal based on multi-scale fuzzy entropy, *Sheng wu yi xue Gong Cheng xue za zhi= Journal of Biomedical Engineering= Shengwu Yixue Gongchengxue Zazhi* 29 (2012) 1184–1188.